

# The TESLA detector

---

**M. Doucet\***

*(for the 2nd ECFA/DESY Study on Physics and Detectors for a Linear  
Electron-Positron Collider)*

*DESY, Hamburg, Germany*

*E-mail: Mathieu.Doucet@desy.de*

ABSTRACT: We present the current design of the detector for the TESLA superconducting linear  $e^+e^-$  collider project in Europe.

---

## 1. Introduction

TESLA (TeV-Energy Superconducting Linear Accelerator) is a project for a superconducting linear  $e^+e^-$  collider. The physics and the detector aspects of this project were the topics of the 2nd ECFA/DESY Study on Physics and Detectors for a Linear Electron-Positron Collider [1]. This collider is intended to have centre-of-mass energies between the mass of the  $Z^0$  and at least 800 GeV. Some parameters of its first 500 GeV stage are shown in table 1. The repetition rate of the collider is 5 Hz, with 2820 bunches per train. The luminosity of the 500 GeV machine is almost three orders of magnitude above LEP, which will allow for a wide physics programme, focusing among other things on Higgs studies, Supersymmetry studies and precision measurements of the Standard Model. More details about the physics programme can be found in the TESLA Technical Design Report [2] and in these proceedings [3]. Details about the current design of the TESLA detector can also be found in the TESLA TDR [4].

## 2. Detector requirements

The TESLA detector will have to perform over a large range of particle energies for complex final states. Several detector requirements have to be fulfilled in order to achieve the physics goals of TESLA. These requirements can be grouped in four categories.

- Tracking: The momentum resolution has to be at least an order of magnitude better than the precision achieved at LEP. The benchmark process in this case is the

---

\*Speaker.

	TESLA	LEP	SLC
Energy [GeV]	500	209	92
Lumi [ $\text{cm}^{-2}\text{s}^{-1}$ ]	$3.4 \times 10^{34}$	$6 \times 10^{31}$	$3 \times 10^{30}$
Bunch spacing [ns]	337	22000	$8.3 \times 10^6$
Beam size (x;y) [nm]	553; 5	$3 \times 10^5$ ; 8000	1500; 650
Bunch length [mm]	0.3	10	1
N/bunch	$2 \times 10^{10}$	$4.5 \times 10^{10}$	$4 \times 10^{10}$

**Table 1:** TESLA accelerator parameters compared to LEP and SLD.

higgsstrahlung process  $e^+e^- \rightarrow Z^0 \rightarrow HZ^0$ . For a decay-independent study of the Higgs, it is important to be able to reconstruct the  $Z^0$  accurately. The requirement for the momentum resolution was set such that the resolution on the measurement of the recoil mass of the  $Z^0$  was given by the intrinsic width of the  $Z^0$ , and not by the resolution of the tracking system. Furthermore, the jet multiplicity and the track density within jets become important at higher energies. The tracking system should be able to resolve tracks in such conditions.

- **Vertex reconstruction:** Vertexing will be important for detailed studies of the Higgs and its decay properties. Since a light Higgs boson has a large decay fraction to  $b\bar{b}$  quarks, flavor tagging will be very important. The vertex detector of TESLA was designed as a multi-layered pixel detector with a minimum amount of material to provide efficient stand-alone tracking and to obtain an impact parameter precision a factor two better than was previously achieved.
- **Energy flow:** Given that most of the interesting signatures at TESLA will appear in hadronic final states, jet reconstruction will be an important issue. The calorimeters must have a high enough granularity to disentangle jets in events with large jet multiplicity. Furthermore, the calorimeters must have a sufficiently good resolution to give a good energy flow reconstruction. The energy flow technique combines the tracking and calorimetry information to obtain an optimal estimate of the energy and direction of partons. Because of the uncertainty on the initial state due to beamstrahlung, and due to the fact that many interesting final states have few kinematical constraints, the energy flow reconstruction is particularly important.
- **Hermeticity:** Since missing energy is the main signature of Supersymmetry and physics processes beyond the Standard Model, the detector should also be as hermetic as possible.

The time structure of the TESLA accelerator justifies a detector with continuous read-out. For most of the components, the data will be processed and compressed at the level of the detector electronics. The data buffered during the bunch trains of about 1 ms will be read out during the long time interval of 200 ms between bunch trains. The event selection will then be done off-line.

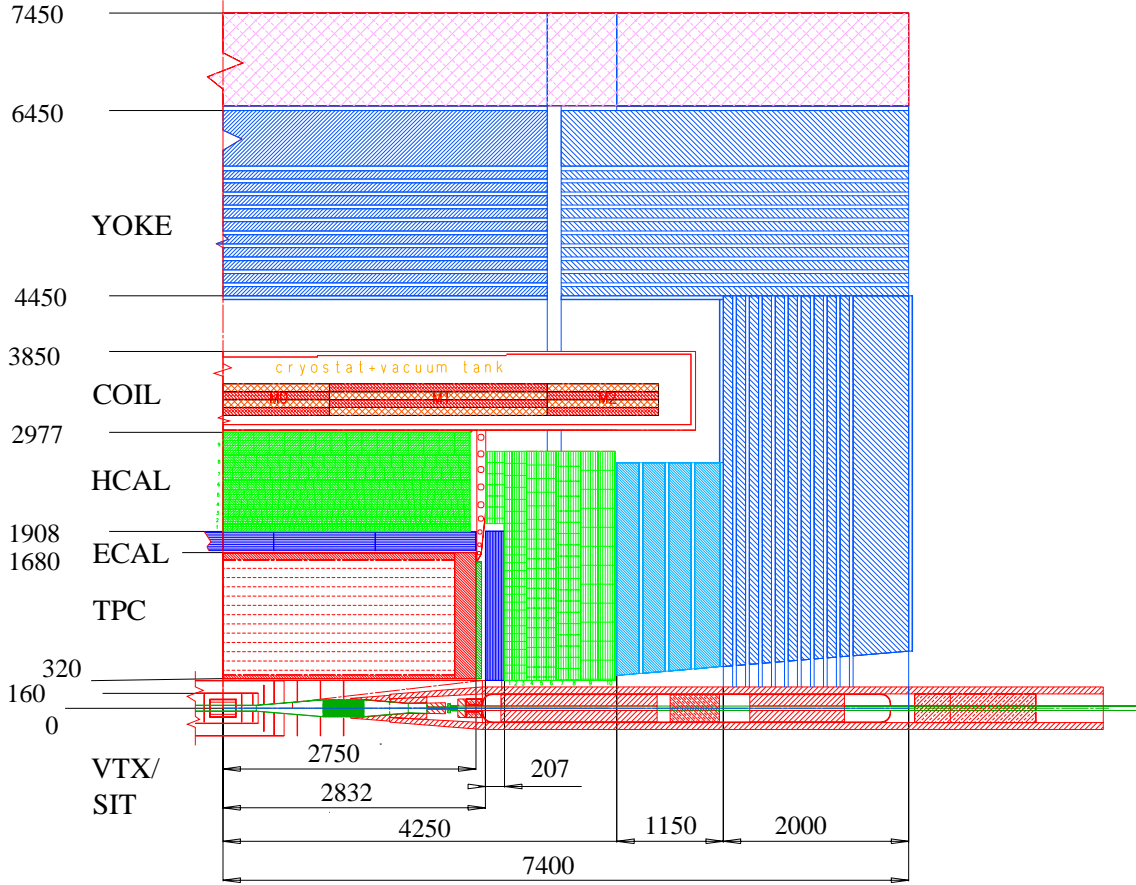


**Figure 1:** Quarter of the TESLA detector. The dimensions are in millimeter.

### 3. Tracking

A large Time Projection Chamber ( $r=170$  cm,  $L=2\times 273$  cm) in a high magnetic field of about 4 Tesla was chosen to provide the required tracking performance. With a large number of measurements along the tracks, the TPC should have a good enough resolution to resolve tracks in a dense environment with multiple jets with high track density. A TPC also has a low density of material, which is an advantage for electron measurements and calorimetry in the detectors surrounding the central tracker.

The TPC is complemented by a multi-layer vertex detector to achieve a good vertex resolution. Between the vertex detector and the TPC, a series of silicon detectors – the Intermediate Tracking System – is placed to improve the track reconstruction efficiency and the matching between the TPC and the VTX detector. The intermediate tracking system extends the track reconstruction down to about  $7^\circ$ . These detectors also provide sufficient precision to identify the bunch crossing for every single track. These silicon detectors and the TPC will be discussed in the following sub-sections.

Although the silicon trackers are designed to minimize the amount of material, the multiple scattering in these detectors can be substantial for very low angle tracks. Furthermore, the TPC resolution becomes very low for low angle tracks, for which the projection

on the TPC end-plate is short. For these reasons, a set of straw-tube planes – the Forward Chambers – is placed parallel to the TPC end-plates on both sides of the TPC. With a resolution of about  $100\ \mu\text{m}$ , these chambers will greatly improve the momentum resolution of low-angle tracks. Apart from assisting the TPC with the tracking, the Forward Chambers can be used to help calibrating the TPC and to serve as a preshower detector for showers initiated in the TPC end-plates.

### 3.1 TPC

The TPC is designed to be as large as necessary to achieve the required performances (see figure 2). Each end-plate has 0.6 million rectangular pads of  $2\times 6\ \text{mm}^2$ . Other pad shapes are also considered. The expected point resolution is about  $150\ \mu\text{m}$  in the transverse direction, with a systematic uncertainty which must be kept below  $10\ \mu\text{m}$ . Each track has an average of about 200 3D-points in the TPC. This TPC would have a tracking efficiency greater than 98%, and a momentum resolution of  $\delta(1/p_T) = 1.4 \times 10^{-4}\ \text{GeV}^{-1}$  in the barrel.

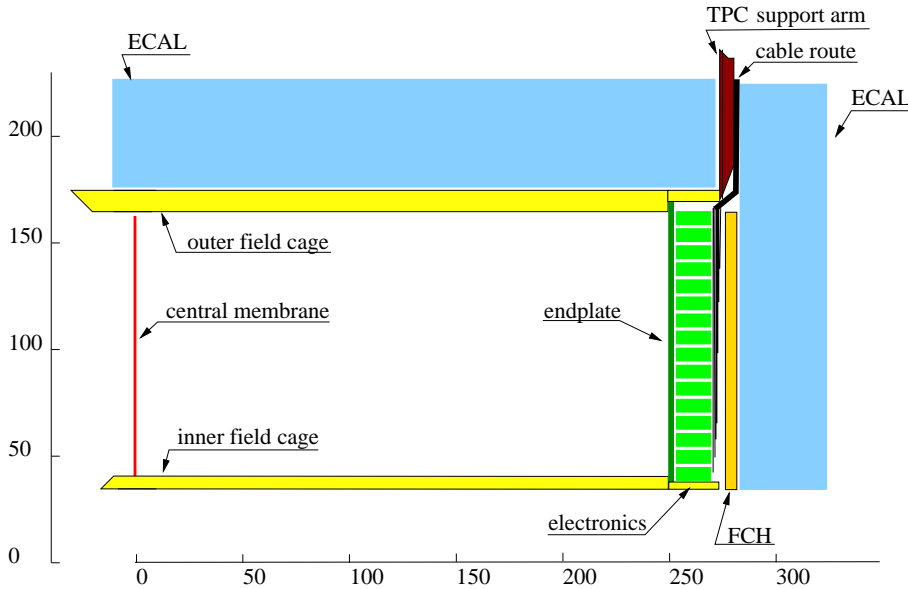


**Figure 2:** Side view of a quarter of the TPC. Dimensions are in centimeters. The Forward Chambers (FCH) near the end-plate of the TPC are also shown.

The TPC will be read out continuously. Since the bunch spacing is relatively short, about 160 bunch crossings will be overlaid during the drift time of about  $55\ \mu\text{s}$ . 160 bunch crossings correspond to about  $0.001\ e^+e^- \rightarrow q\bar{q}$  events. A readout speed of 20 MHz should be sufficient to disentangle the bunch crossings. Further timing precision will be provided by the vertex detector and the intermediate tracking system.

The continuous data taking of the TPC also has implications on the readout technology. It is foreseen to use GEMs [5] instead of the traditional MWPC readout. GEMs have the advantage of being more uniform and of naturally reducing the  $E \times B$  effect and the ion feedback. Since the ions travel only about 1 cm during a bunch train, a gating GEM

placed 2 cm upstream of the end-plate could be used if the ion feedback suppression of GEMs proves to be insufficient. A voltage difference of 50 V through the gating GEM could be switched on and off between bunch trains. Other options for the TPC readout are micromegas and MWPC.

### 3.2 Vertex detector

To maximize the resolution, the vertex detector has been designed to be as close as possible to the beam pipe and to have the least amount of material while having a maximal lever arm. One of the options of the current design foresees five layers of CCD detectors to provide an efficient stand-alone tracking. The radius of the first CCD layer is 15 mm, one millimeter away from the beam pipe. The outer layer has a radius of 60 mm. The three inner layers cover an angular range down to  $|\cos\theta| = 0.96$  and tracks hitting all the five layers are possible down to  $|\cos\theta| = 0.9$ .

The beam related background on the first layer is estimated to be 0.03 hits/mm<sup>2</sup> per bunch crossing. A CCD detector with 20×20 μm<sup>2</sup> pixels would be appropriate if it can be completely read out fast enough to keep the hit density sufficiently low. To reach this speed, a 50MHz readout chip must be developed to read out the first CCD layer within 50 μs. In its present version, the complete vertex detector has 800 million channels.

In order to minimize the amount of material, the detector is planned to be built out of stretched CCD ladders. The material could then be reduced to about 0.06 X<sub>0</sub> per layer, in addition to a thin Beryllium support of 1.1 X<sub>0</sub> near the beam pipe. With the current design, the vertex detector would have a resolution of  $\sigma(\text{IP})_{r\phi} = 4.19\mu\text{m} \oplus 4.00\mu\text{m}/(p \sin^{3/2}\theta)$ , which is a factor two better than what was achieved by SLD with CCD technology [6]. Other options for the vertex detector are CMOS detectors and hybrid pixels.

### 3.3 Intermediate tracking system

A set of silicon detectors will be built between the TPC and the vertex detector to improve the momentum resolution by adding a few precise points at a relatively large distance from the primary interaction point. These detectors will also help the matching of tracks between the TPC and the vertex detector. This Intermediate Tracking System, shown in figure 3, consists of two cylinders of double-sided strip detectors at R=16 cm and R=30 cm (the Silicon Intermediate Tracker – SIT), and seven disks of silicon detectors perpendicular to the beam axis on each side of the interaction point (the Forward Tracker – FTD). The three disks closest to the interaction point are made of silicon pixels and the four others are made of strip detectors. While the two cylinders provide a resolution of about 10 μm in r-φ, the requirement on the disks is only of the order of 25 μm.

### 3.4 Tracking performance

The overall efficiency of the tracking system is above 98% for particles above 1 GeV. This efficiency drops to about 95% in the forward region. Figure 4 shows the momentum resolution of the TESLA detector, with the contributions from the different subdetectors. The intermediate tracking system improves the momentum resolution by 30% in the barrel region when added to the TPC and vertex detector information. It also extends the

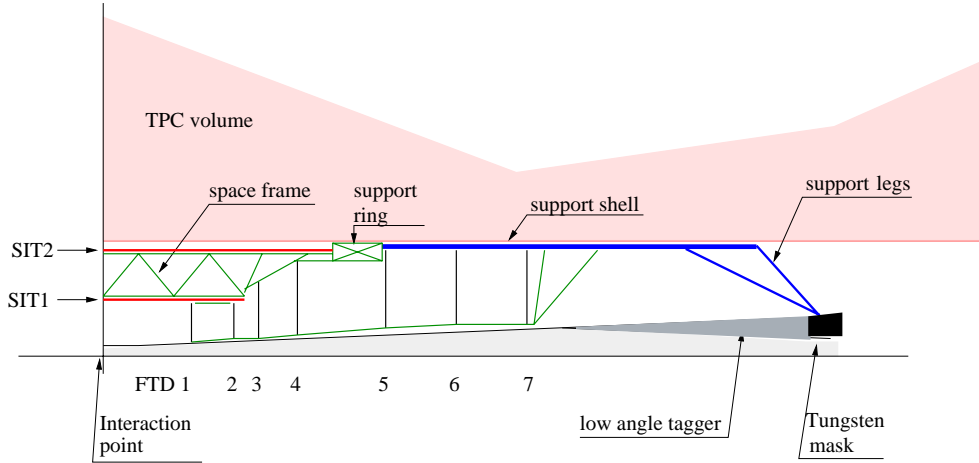


**Figure 3:** Intermediate tracking system.

detection of tracks down to about  $7^\circ$ . The forward chambers on each side of the TPC help improving the momentum resolution by a substantial factor in the low angle region. The momentum resolution in the barrel region is  $\delta(1/p_T) = 5 \times 10^{-5} \text{ GeV}^{-1}$ , which is a factor 10 better than what was achieved at LEP by ALEPH [7]. The resolution goes down to about  $\delta(1/p_T) = 3 \times 10^{-4} \text{ GeV}^{-1}$  at low angle.

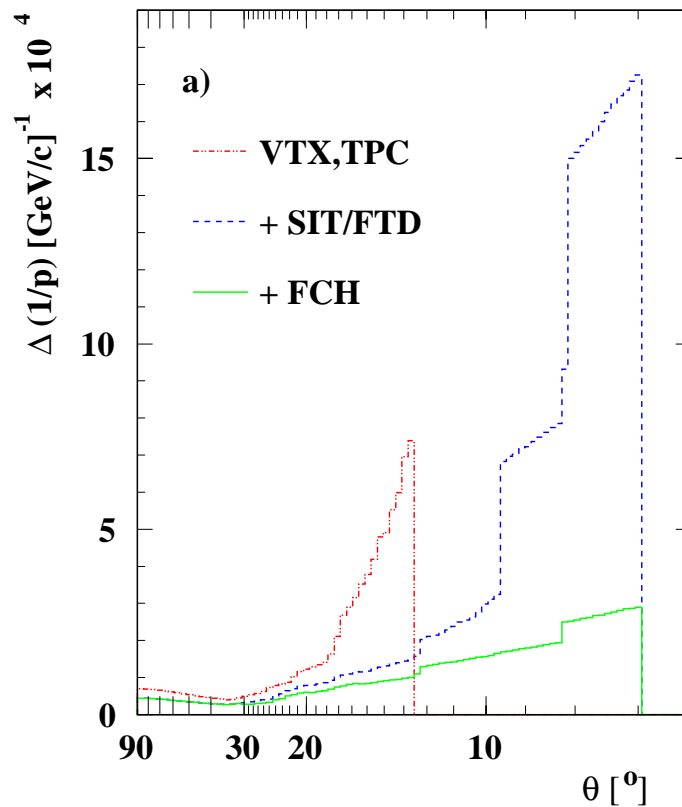


**Figure 4:** Momentum resolution as a function of the angle.

Flavor tagging will be of prime importance for many physics studies at TELSA, for example to identify b-quarks in Higgs decays. Figure 5 shows the purity of b- and c-tagging as a function of the efficiency. Thanks to the small amount of material of the vertex detector, the b-tagging purity remains above 90% for efficiencies up to 80% and a c-tagging purity of about 90% can be reached with an efficiency of 30%.

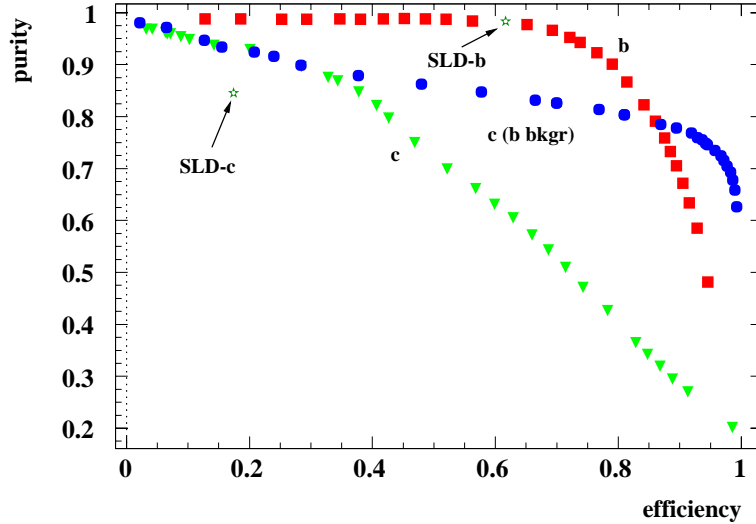


**Figure 5:** Efficiency versus purity of the b- and c-tagging for jets from  $Z^0$  decays.

## 4. Calorimetry

Both the electromagnetic and hadronic calorimeters will be highly segmented. The high granularity is necessary to disentangle multi-jet events and to provide a good angular and energy resolution of jets. The calorimeters must in addition have a sufficiently good timing to avoid event pile-up. To diminish the amount of material in front of the calorimeters, these will be placed inside the coil, which is  $1.6 \lambda$  deep.

### 4.1 Electromagnetic calorimeter

The electromagnetic calorimeter is planned to be a large highly segmented silicon/tungsten detector. The detector elements are  $1 \times 1 \text{ cm}^2$  silicon cells interleaved with 1.4 mm of tungsten. The tungsten also serves as the supporting structure of the calorimeter. The electromagnetic calorimeter has a total of 32 million channels.

The energy resolution estimated with the current design is  $\delta E/E = 13\%/\sqrt{E(\text{GeV})}$ , which is similar to what was achieved with the ALEPH detector [7]. The angular resolution for photons is on the other hand much higher. It is estimated at  $\delta\theta = 0.63/\sqrt{E(\text{GeV})} \oplus 0.24 \text{ mrad}$ , which is to be compared with  $\delta\theta = 2.5/\sqrt{E(\text{GeV})} \oplus 0.25 \text{ mrad}$  achieved by ALEPH.

Another option for the electromagnetic calorimeter would be based on a shashlik structure, with wavelength shifting fibres running through towers of scintillator tiles. A shashlik

calorimeter using scintillators with different time constants is also considered in order to obtain a longitudinal profile of the showers. Interleaving shashlik towers by planes of small silicon pads can also be envisaged to improve the granularity of the calorimeter.

#### 4.2 Hadronic calorimeter

The hadronic calorimeter design is optimized to measure energy depositions with a resolution sufficient to achieve the energy flow requirements. The main option is a highly granular scintillator tile detector with wavelength shifting fibre readout. The smallest tiles are of the order of  $5 \times 5 \text{ cm}^2$ . The cells are interleaved by 20 cm of iron ( $4.5 \lambda$ ) in the barrel and in the endcap regions to offer a good longitudinal sampling. The hadronic calorimeter has 200000 channels.

The energy resolution of the detector is estimated to be about  $\delta E/E = 35\%/\sqrt{E(\text{GeV})} \oplus 3\%$ , which can be compared to  $\delta E/E = 85\%/\sqrt{E(\text{GeV})}$  achieved by ALEPH [7].

Another option for the hadronic calorimeter would be a so-called “digital” calorimeter. It would be a highly granular detector with a small cell size of the order of a centimeter. By counting the amount of hit cells one could measure the deposited energy. Wire chambers could for instance be used for this purpose.

#### 4.3 Energy flow performance

The energy flow reconstruction should provide an important measurement of the energy and direction of partons. An optimal estimate of the energy flow requires the combination of the information obtained from both the trackers and the calorimeters. The central tracking detectors are used to reconstruct charged particles, the electromagnetic calorimeter is used to reconstruct photons, and long lived neutral hadrons are reconstructed by the hadronic calorimeter.

The energy flow performance goal of TESLA is around  $\delta E/E = 30\%/\sqrt{E(\text{GeV})}$ . This can be compared with the energy flow performance of the ALEPH detector [7]  $\delta E/E = 60\%(1 + |\cos \theta|)/\sqrt{E(\text{GeV})}$ . The performance can be appreciated by studying the self-coupling process of the Higgs [8]  $e^+e^- \rightarrow Z^0 \rightarrow Z^0H \rightarrow Z^0HH \rightarrow 6 \text{ jets}$ . Figure 6 shows the distribution of the variable defined as follows:

$$Dist = [(m_{12} - m_h)^2 + (m_{34} - m_h)^2 + (m_{56} - m_Z)^2]^{1/2}, \quad (4.1)$$

where  $m_{12}, m_{34}$  and  $m_{56}$  are the invariant masses of pairs of jets and  $m_h$  and  $m_Z$  are the masses of the Higgs and the  $Z^0$ . The simulated distributions for the TESLA detector and for a LEP-like detector with the performance stated above are compared for  $m_h = 120 \text{ GeV}$ ,  $\sqrt{s} = 500 \text{ GeV}$  and an integrated luminosity of  $500 \text{ fb}^{-1}$ . The TESLA detector can be seen to distinguish significantly better between signal and background compared to a LEP detector. The results of such an analysis underline the fact that a good granularity is very important for the TESLA detector.

### 5. Forward region

The high luminosity and the small beam size of the TESLA accelerator cause the electrons and positrons in the beams to feel each other’s electromagnetic field. This *beamstrahlung*

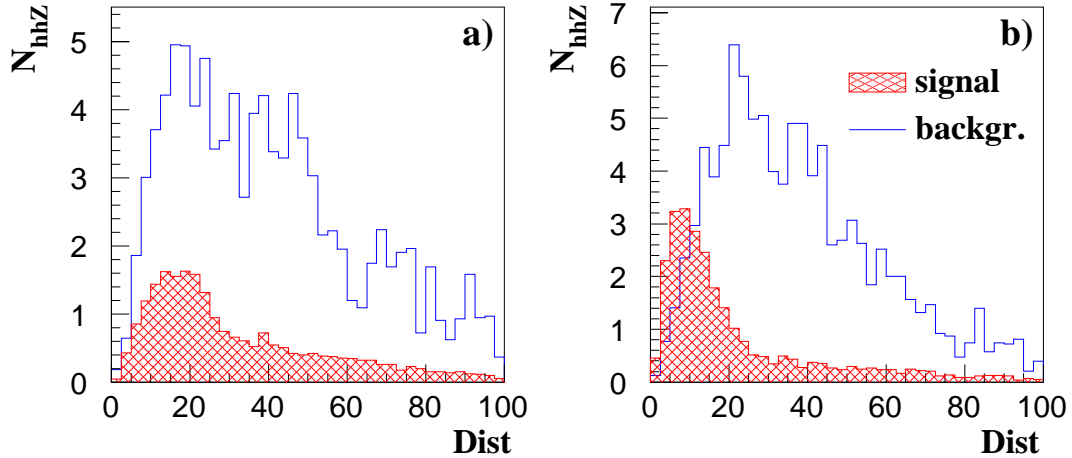


**Figure 6:** Influence of the energy flow resolution on the self-coupling study of the Higgs. Left: Performance of a LEP-like detector. Right: Performance of the TESLA detector.

effect will produce a large amount of photons and electrons at low angle, which could hit beam elements and create a large background in the detector if not shielded. For this reason, a large tungsten shield has been designed on both sides of the detector to absorb both the photons and electrons from the beamstrahlung and potential background particles created along the beam line.

This shield will be instrumented by two calorimeters. A first calorimeter, the Low-Angle Tagger, is a silicon/tungsten detector which covers the angular range between 27 mrad and 83 mrad. It is subdivided in 63 planes of silicon diode and 2 mm of tungsten ( $0.6 X_0$ ). Each plane is subdivided in 7 layers in  $r$  and 24 sectors in  $\phi$ . The estimated resolution of the LAT is  $\delta E/E = 20 - 25\%/\sqrt{E(\text{GeV})}$ .

The second calorimeter, the Luminosity Calorimeter, covers the angular range between 5.5 mrad and 28 mrad, with a structure similar to the LAT. This detector will also be used to measure the relative luminosity between bunches. By measuring the signal from the beamstrahlung background, this detector will be used in a fast-feedback system of the accelerator. Due to the very large electromagnetic radiation near the beam, a diamond/tungsten detector is considered. Placed only 1.2 cm from the beam, this detector could received as much as a few MGy of electromagnetic radiation per year. Diamond detectors have been extensively studied in the past years for applications at the LHC. They have also recently been tested at DESY for electromagnetic radiation hardness up to 10 MGy [9].

## 6. Conclusion

The wide physics programme of TESLA will require the construction of a very performant detector. The detector design of the 2nd ECFA/DESY Study on Physics and Detectors for a Linear Electron-Positron Collider should meet the performance requirements. Research and Development programmes are already underway to meet the current design goals.

## References

- [1] <http://www.desy.de/conferences/ecfa-desy-lc98.html>
- [2] TESLA TDR part III, *The TESLA Physics Programme*, editors: R.-D. Heuer, D. Miller, F. Richard, P. Zerwas, DESY 2001-011, 2001.
- [3] W. Menges, these proceedings.
- [4] TESLA TDR part IV, *A Detector for TESLA*, editors: T. Behnke, S. Bertolucci, R.-D. Heuer, R. Settles, DESY 2001-011, 2001.
- [5] F. Sauli, Nucl. Instr. and Meth. A386 (1997) 531.
- [6] K. Abe et al., Nucl. Instr. and Meth. A400 (1997) 287.
- [7] D. Buskulic et al., Nucl. Instr. and Meth A360 (1995) 481.
- [8] C. Castanier et al., *Higgs self coupling measurement in  $e^+e^-$  collisions at center-of-mass energy of 500 GeV*, hep-ex/0101028 (2000).
- [9] T. Behnke et al., *Electromagnetic radiation hardness of diamond detectors*, hep-ex/0108038 (2001).